Research Article

RIS-AIDED MULTI-ANTENNA IOT SYSTEMS: PERFORMANCE EVALUATION UNDER MRC COMBINING

Thien P. $NGUYEN^1$, Dinh Tung VO^2 , Quang-Sy VU^3 , Minh $TRAN^3$, Quang-Sang $NGUYEN^{4,*}$, Taejoon KIM^5

¹Faculty of Electrical and Electronics Engineering, Ton Duc Thang University, Ho Chi Minh City, Vietnam ²HUTECH Institute of Engineering, HUTECH University, Ho Chi Minh City, Vietnam ³Advanced Intelligent Technology Research Group, Faculty of Electrical and Electronics Engineering, Ton Duc Thang University, Ho Chi Minh City, Vietnam

⁴Posts and Telecommunications Institute of Technology, Ho Chi Minh City, Vietnam ⁵School of Information and Communication Engineering, Chungbuk National University, Cheongju-si, South Korea

 $42100891@student.tdtu.edu.vn,\ vd.tung@hutech.edu.vn,\ vuquangsy@tdtu.edu.vn,\ tranhoangquangminh@tdtu.edu.vn,\ sangnq@ptit.edu.vn,\ ktjcc@chungbuk.ac.kr$

*Corresponding author: Sang-Quang Nguyen; sangnq@ptit.edu.vn

DOI: 10.15598/aeee.v23i3.250801

Article history: Received Aug 1, 2025; Revised Aug 18, 2025; Accepted Sep 19, 2025; Published Sep 30, 2025.

This is an open access article under the BY-CC license.

Abstract. Reconfigurable Intelligent Surfaces (RISs) have emerged as a promising solution for future wireless communication systems due to their ability to reconfigure the radio propagation environment in a cost and energy efficient manner. This study focuses on the performance of RIS assisted wireless systems where the receiver is equipped with multiple antennas and employs receive diversity techniques, specifically Maximal Ratio Combining (MRC), over Rayleigh fading channels. We derive new closed form expressions for the outage probability (OP) by modeling the signal to noise ratio (SNR) as a Gamma distributed random variable. To validate the analytical expressions, Monte Carlo simulations are conducted and demonstrate a high level of agreement with the theoretical analysis. The obtained results offer useful insights into the efficient integration of RIS and antenna diversity for enhancing link reliability under severe fading conditions.

Keywords

Reconfigurable Intelligent Surface, maximal ratio combining, receive diversity, gamma approximation.

1. Introduction

The growing demand for ultra reliable and high capacity wireless communication has motivated the development of novel approaches that can reconfigure the wireless propagation environment. Reconfigurable Intelligent Surfaces (RIS), also referred to as Intelligent Reflecting Surfaces (IRS), have emerged as a promising technology for future wireless systems such as 5G and even beyond, including 6G networks [1–6]. By utilizing large arrays of nearly passive reflecting elements, RIS can actively control the propagation of electromagnetic waves through adjustable phase shifts, enabling both energy efficient and spectrum efficient smart radio environments. The deployment of RIS in various communication architectures has attracted significant research interest in recent years. For example, the integration of RIS with relay-assisted systems is investigated in [7–10], while its application in non-orthogonal multiple access (NOMA) scenarios is studied in [11–13], with particular emphasis on RIS-enabled short packet NOMA systems [14]. Furthermore, RIS-assisted satellite communication networks have also been considered as a key research direction [15–18]. In addition, the performance evaluation of systems employing multiple RISs has been presented in [19–21].

However, most existing works are based on analytical approximations or simulation-based evaluations, which provide limited insights into the fundamental statistical characteristics of RIS assisted wireless channels [22, 23]. Deriving exact expressions for key performance metrics such as the cumulative distribution function (CDF), outage probability, and achievable system capacity remains a significant challenge due to the composite nature of signal fading introduced by RIS. The adoption of generalized statistical fading models, including the Gamma, exponential, and beta distributions, offers enhanced modeling flexibility but introduces additional complexity to the analytical framework [24, 25].

In this work, we present a comprehensive analytical performance evaluation of RIS assisted wireless communication systems employing diversity techniques under generalized fading conditions. A closed-form expression for CDF of the end-to-end signal to noise ratio (SNR) is derived, which enables an accurate assessment of the outage probability. The analytical results are validated through extensive Monte Carlo simulations. In addition, a detailed parameter sensitivity analysis is carried out to provide practical design guidelines for RIS based systems. The main contributions and novelties of this work are summarized as follows:

- We consider a RIS-assisted wireless communication system over Rayleigh fading channels, where the destination is equipped with K receive antennas and employs maximal ratio combining (MRC) for signal detection. Departing from the ideal phase-shift assumption commonly used in existing studies, we incorporate practical phase errors stemming from quantization to better reflect realworld system behavior.
- A closed-form expression for the outage probability is derived by approximating the end-to-end SNR distribution using the Gamma model, which provides analytical tractability.
- The influence of key system parameters, including the transmit power to noise ratio (P_S/σ^2) , the number of receive antennas K, the number of RIS elements, and the transmission rate R, on system performance is thoroughly investigated.
- The accuracy of the derived analytical expressions is confirmed by Monte Carlo simulations, which show excellent agreement with the theoretical predictions.
- The developed framework offers valuable insights into the diversity gains achievable through antenna array configurations and intelligent signal reflection in RIS assisted communication scenarios.

The remainder of this paper is organized as follows. Section 2. describes the system architecture and the main assumptions adopted in the analysis. In Section 3. , the statistical behavior of the wireless channel is characterized, and closed form expressions for the outage probability and the diversity order are derived. Section 4. presents numerical simulation results that verify the analytical findings and provide further performance insights. Finally, Section 5. concludes the paper and discusses possible directions for future research.

2. System Model

In this paper, we consider a wireless communication system in which a source node S transmits data to a destination node D, which is equipped with K receive antennas, indexed by the set $\mathcal{K} = \{1, 2, \ldots, K\}$. To enhance the system performance, RIS is deployed to assist the communication process, as illustrated in Fig. 1. The RIS consists of N passive reflecting elements, indexed by the set $\mathcal{N} = \{1, 2, \ldots, N\}$, and is controlled by a dedicated controller capable of dynamically adjusting the phase shift of each element to optimize the signal combination at the receiver.

The entire system is assumed to operate in a statistically homogeneous environment, where all wireless links experience independent Rayleigh fading. The received signal at the k-th antenna of the destination node comprises two components: the direct link from the source $(S \to D_k)$ and the reflected link assisted by the RIS $(S \to RIS \to D_k)$. Hence, the overall received signal can be expressed as follows:

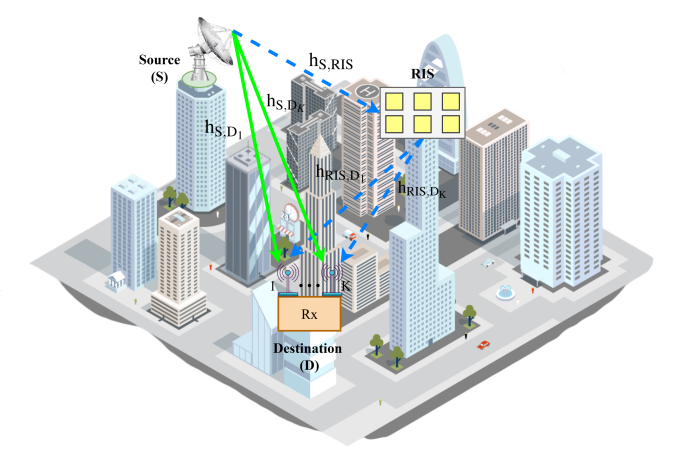


Fig. 1: System model.

$$y_{D_k} = \sqrt{P_S} x_S \left(h_{S,D_k} + h_{\text{RIS},D_k}^T \Phi h_{S,\text{RIS}} \right) + z_{D_k}, \quad (1)$$

where x_S denotes the unit power information symbol transmitted by the source node, P_S is the transmit power of the source, and z_{D_k} represents the additive white Gaussian noise (AWGN) at the k-th receive antenna, with zero mean and variance σ^2 . The coefficients h_{S,D_k} , $h_{S,RIS}$, and h_{RIS,D_k} represent the channel coefficients from the source to D_k , from the source to the RIS, and from the RIS to D_k , respectively.

The matrix $\Phi = \operatorname{diag}(\alpha_1 e^{j\theta_1}, \dots, \alpha_N e^{j\theta_N})$ denotes the diagonal reflection coefficient matrix of the RIS, where $\alpha_n \in (0, 1]$ is the amplitude reflection coefficient and $\theta_n \in [0, 2\pi)$ is the phase shift of the *n*-th element. The notation $e^{(\cdot)} = \exp(\cdot)$ represents the exponential function, and $(\cdot)^T$ denotes the transpose operation.

Based on (1), the instantaneous signal to noise ratio (SNR) at the k-th receive antenna is given by

$$\gamma_{D_k} = \frac{P_S \left\| h_{S,D_k} + h_{\text{RIS},D_k}^T \Phi h_{S,\text{RIS}} \right\|^2}{\sigma^2}, \qquad (2)$$

where $\|\cdot\|$ denotes the Euclidean norm.

In practical RIS implementations, perfect phase control at each element is often unattainable due to hardware limitations, as discussed in [26,27], and the effects of phase imperfections are further examined in [28,29]. In this work, we specifically consider the impact of quantization resolution. Instead of applying an ideal continuous phase shift, each RIS element can only produce discrete phase values, resulting in undesired phase errors. It is assumed that the phase error Θ_n at the n-th RIS element follows a uniform distribution over the interval $\left[-\frac{\Delta}{2},\frac{\Delta}{2}\right]$, where $\Delta=\frac{2\pi}{2^q}$, and q denotes the number of quantization bits.

The probability density function (PDF) of Θ_n is given as follows:

$$f_{\Theta_n}(x) = \begin{cases} \frac{1}{\Delta}, & x \in \left[-\frac{\Delta}{2}, \frac{\Delta}{2}\right], \\ 0, & \text{otherwise.} \end{cases}$$
 (3)

Assuming the ideal phase shift is θ_{ideal} , the actual phase applied at the RIS element is modeled as $\theta_n = \theta_{\text{ideal}} - \Theta_n$.

3. Performance Analysis

This section presents a comprehensive analysis of the system performance by applying MRC at the destination node. Under the MRC technique [30], the destination combines the received signals from all antennas to maximize the instantaneous SNR. Mathematically,

the resulting SNR can be expressed as follows:

$$\gamma_{\text{MRC}} = \sum_{k=1}^{K} \gamma_{D_k}, \tag{4}$$

where γ_{D_k} represents the instantaneous SNR observed at the k-th antenna of the destination.

3.1. Outage Probability of the System

Outage probability (OP) is a key metric for evaluating the performance of wireless communication systems [31, 32]. It quantifies the probability that the instantaneous SNR falls below a predefined threshold, resulting in a communication failure.

Mathematically, the outage probability corresponds to CDF of the instantaneous SNR γ , and is given by:

$$F_{\gamma}(\gamma_{\rm th}) = \Pr\left(\gamma < \gamma_{\rm th}\right)$$

$$= \Pr\left(\frac{P_S}{\sigma^2} ||Z||^2 < \gamma_{\rm th}\right)$$

$$= \Pr\left(Z < \sqrt{\frac{\gamma_{\rm th}\sigma^2}{P_S}}\right),$$
(5)

where $Z = \sum_{k=1}^{K} z_k$, and $\gamma_{\rm th} = 2^R - 1$ denotes the minimum SNR required to support the target transmission rate R.

3.2. Gamma Approximation Method

Since the exact expression of $F_Z(z)$ is analytically intractable, we adopt the moment matching method to approximate its distribution using the Gamma distribution. The approximate CDF of Z is given by [6]:

$$F_Z(z) \approx \frac{\gamma(\alpha, \beta z)}{\Gamma(\alpha)},$$
 (6)

where $\gamma(\cdot, \cdot)$ is the lower incomplete Gamma function, defined as:

$$\gamma(a,x) = \int_0^x t^{a-1}e^{-t} dt,$$

and $\Gamma(a)$ is the complete Gamma function, given by:

$$\Gamma(a) = \int_0^\infty t^{a-1} e^{-t} dt.$$

The shape parameter α and the rate parameter β are determined by matching the first and second order moments of z_k , as follows:

$$\alpha = \frac{\left(\mathrm{E}\{Z\}\right)^2}{\mathrm{Var}\{Z\}}, \quad \beta = \frac{\mathrm{E}\{z_k\}}{\mathrm{Var}\{z_k\}},\tag{7}$$

where $E\{Z\}$ denotes the expected value (mean) of Z, and $Var\{Z\}$ is its variance, representing the dispersion of Z around the mean.

3.3. Maximal Ratio Combining (MRC)

We assume that perfect channel state information (CSI) is available at the destination for all relevant links, including the direct source-to-destination channels (h_{S,D_k}) as well as the cascaded source-to-RIS $(h_{S.RIS})$ and RIS-to-destination (h_{RIS,D_k}) channels. This enables the implementation of MRC and allows for accurate coherent combining of signals. At the RIS, only quantized phase adjustments are assumed to be feasible, and the phase shifts θ_n are configured by an external controller that relies on the CSI estimated at the destination. Since the RIS operates passively, it does not perform local channel estimation; instead, the optimized phase configuration is fed back to the RIS through a low-rate control link.

It is important to emphasize that this assumption of perfect CSI at the destination represents an idealized benchmark. In practical deployments, CSI acquisition may suffer from estimation errors, feedback latency, and hardware impairments, which would inevitably degrade the achievable performance. Nevertheless, adopting perfect CSI in the analysis provides a tractable framework for deriving closed-form expressions and characterizing the theoretical upper bounds of RIS-assisted MRC systems.

Lemma 1. The expected value of Z is given by:

$$\mathrm{E}\{Z\} = K\left(\sigma\sqrt{\frac{\pi}{2}}\right) + K \times N \times \left(\sigma\sqrt{\frac{\pi}{2}}\right)^2 \times \mathrm{sinc}\left(\frac{\Delta}{2}\right), Proof. \text{ A detailed proof is provided in Appendix A.} \quad \Box$$
(8)

where the function sinc(x) denotes the normalized sinc function, defined as:

$$\operatorname{sinc}(x) = \frac{\sin(x)}{x}, \quad \text{for } x \neq 0, \quad \operatorname{sinc}(0) = 1.$$

Proof. A detailed proof is provided in Appendix A.

Lemma 2. The variance of Z is expressed as follows:

$$\operatorname{Var}\{Z\} = K \left(2\sigma^2 - \left(\sigma\sqrt{\frac{\pi}{2}}\right)^2\right) + K \times N$$
$$\times \left(4\sigma^4 \operatorname{sinc}\left(\Delta\right) - \left(\sigma\sqrt{\frac{\pi}{2}}\right)^4 \operatorname{sinc}\left(\frac{\Delta}{2}\right)^2\right). \tag{9}$$

Proof. A detailed proof is provided in Appendix A. \square mit power-to-noise ratio, P_s/σ^2 (in dBm), for both

3.4. Random Antenna Selection (Ran)

We now investigate the Random Antenna Selection (Ran) scheme. Unlike selection combining or maximum ratio combining, the receiver does not rely on CSI to determine the best antenna. Instead, one receive antenna is randomly chosen from the total set of K available antennas, and this antenna remains fixed for the corresponding transmission block. This scheme serves as a baseline reference to evaluate the performance gain of more sophisticated combining techniques.

The resulting received signal can be expressed as

$$Z = h_{S,D_k} + \sum_{n=1}^{N} h_{S,RIS} \exp(j\theta_n) h_{RIS,D_k},$$

with $k \in \{1, 2, \dots, K\}$.

Lemma 3. The expected value of Z is given by:

$$E\{Z\} = \sigma \sqrt{\frac{\pi}{2}} + N \times \left(\sigma \sqrt{\frac{\pi}{2}}\right)^2 \times \operatorname{sinc}\left(\frac{\Delta}{2}\right).$$
 (10)

Proof. A detailed proof is provided in Appendix A. \Box

Lemma 4. The variance of Z is expressed as follows:

$$\operatorname{Var}\{Z\} = \left(2\sigma^2 - \left(\sigma\sqrt{\frac{\pi}{2}}\right)^2\right) + N$$

$$\times \left(4\sigma^4\operatorname{sinc}(\Delta) - \left(\sigma\sqrt{\frac{\pi}{2}}\right)^4\operatorname{sinc}\left(\frac{\Delta}{2}\right)^2\right). \tag{11}$$

4. Simulation Results

In this section, we perform Monte Carlo simulations (denoted as Sim) to validate the accuracy of the derived outage probability expressions (denoted as **Theo**). The Monte Carlo method is widely used in modern scientific research, enabling objective and accurate assessment of system performance under various conditions. Unless otherwise specified in the individual figures, the default simulation parameters are set as follows: the number of reflecting elements at the RIS is N = 4, data rate R = 1 bit/s/Hz, transmit power to noise variance ratio $\frac{P_S}{\sigma^2} = 2$ dBm, number of receive antennas K=4, phase quantization resolution q=3 bits, and the number of Monte Carlo trials is 10^6

Figure 2 presents the OP as a function of the trans-

MRC and Ran schemes. It is observed that the OP decreases monotonically with increasing P_s/σ^2 , validating the expected performance gain at higher transmit power levels. Specifically, the MRC scheme achieves a significantly steeper decline in OP and approaches nearly zero, thereby ensuring a high level of link reliability. In contrast, the Ran scheme exhibits a slower convergence, resulting in a noticeable performance gap compared to MRC. Moreover, the theoretical curves are in close agreement with the simulated counterparts, which demonstrates the accuracy of the analytical derivations. The minor discrepancy can be attributed to approximation techniques in the theoretical analysis, such as the Gamma distribution fitting, which introduce slight deviations from the simulation outcomes.

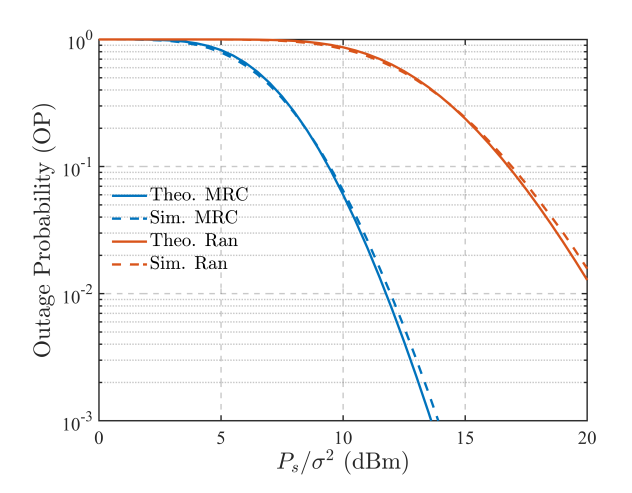


Fig. 2: OP vs. the normalized transmit power.

Figure 3 shows the OP as a function of the number of RIS elements, N, for both MRC and Ran schemes. It is observed that the OP of the MRC scheme decreases rapidly and approaches zero when $N \geq 4$, indicating that only a moderate number of reflecting elements are

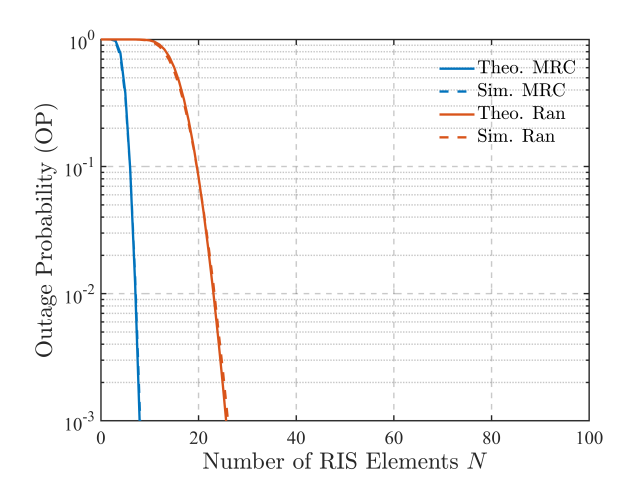


Fig. 3: OP vs. number of elements.

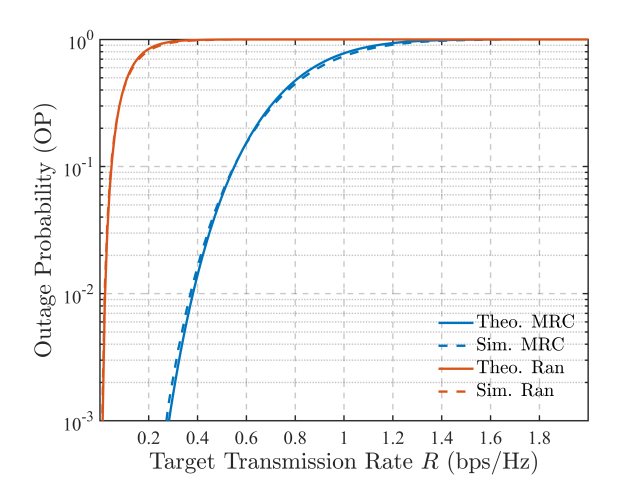


Fig. 4: OP vs. the target transmission rate.

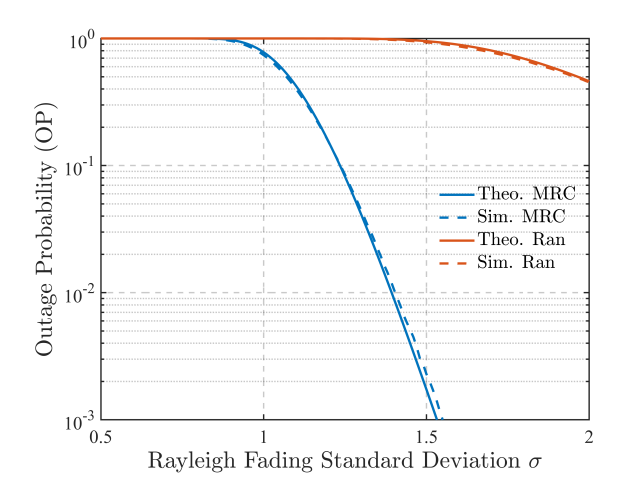


Fig. 5: OP vs. the Rayleigh fading standard deviation.

sufficient to achieve reliable performance. In contrast, the Ran scheme requires a much larger number of elements $(N \geq 20)$ to attain a comparable OP level, reflecting its lower efficiency. Moreover, the theoretical and simulation results are in close agreement for both schemes, confirming the validity of the analytical models. The evident performance gap highlights the importance of optimal phase design in fully exploiting the RIS-assisted system.

Figure 4 depicts the OP as a function of the target transmission rate, R (bps/Hz), for both MRC and Ran schemes. As expected, the OP increases with R, since higher data rates require stronger channel conditions to maintain reliable communication. It is observed that the MRC scheme provides a much lower OP across the entire range of R, maintaining values below 10^{-2} for moderate rates (e.g., $R \leq 0.8$ bps/Hz). In contrast, the Ran scheme suffers from a steep rise in OP, approaching unity even at relatively low rates, which indicates its inefficiency in supporting high spectral efficiency. Furthermore, the excellent agreement

between theoretical and simulated results validates the accuracy of the analytical framework. Overall, these results highlight the robustness of MRC in accommodating higher transmission rates compared to Ran.

Finally, Figure 5 illustrates the variation of the OP with respect to the Rayleigh fading standard deviation σ for two different reception strategies: MRC and Ran. It can be observed that as σ increases, the OP of both schemes decreases, but with significantly different rates. Specifically, for MRC, the Theo and Sim curves match closely, confirming the accuracy of the analytical expressions and highlighting the superior performance of MRC in exploiting diversity. In contrast, the random selection scheme exhibits much worse performance, as the outage probability remains relatively high even at larger values of σ , indicating its inability to leverage spatial diversity effectively. These results emphasize that MRC is a much more efficient strategy for enhancing system reliability under Rayleigh fading conditions.

5. Conclusion

This study investigates the performance of a wireless communication system assisted by reconfigurable intelligent surfaces under practical conditions with phase estimation errors, which are modeled using a uniform distribution. A closed-form expression for the outage probability is derived by approximating the signal-to-noise ratio with a Gamma distribution. The analysis is conducted in the context of a receiver equipped with multiple antennas employing maximal-ratio combining over independent Rayleigh fading channels. Monte Carlo simulations are provided to validate the theoretical expressions, demonstrating a close match.

The results indicate that integrating RIS with antenna diversity at the receiver is an effective approach to enhancing link reliability, even in the presence of phase mismatches. This work contributes a practical perspective for the implementation of RIS in next-generation wireless communication systems.

Future work will extend this study by considering alternative receive diversity techniques such as selection combining, as well as investigating the channel capacity of the system. Deriving a closed-form expression for the channel capacity remains a significant challenge and will be a focal point of subsequent research.

Acknowledgment

This research is supported by Posts and Telecommunications Institute of Technology (PTIT).

Author Contributions

T.P.Nguyen proposed the system model, D-T.V and Q-S.V performed the analytic calculations, while M.Tran and Q-S.Nguyen performed the numerical simulations. All authors contributed to the final version of the manuscript. K.Taejoon supervised the project.

References

- LE, A.-T., T. N. NGUYEN, L.-T. TU, T.-P. TRAN, T. T. DUY, M. VOZNAK and Z. DING. Performance Analysis of RIS-Assisted Ambient Backscatter Communication Systems. *IEEE Wireless Communications Letters*. 2024, vol. 13, iss. 3, pp. 791–795. ISSN 2162-2337. DOI: 10.1109/LWC.2023.3344113.
- [2] WU, Q. and R. ZHANG. Intelligent Reflecting Surface Enhanced Wireless Network via Joint Active and Passive Beamforming. *IEEE Transactions on Wireless Communications*. 2019, vol. 18, iss. 11, pp. 5394–5409. ISSN 1536-1276. DOI: 10.1109/TWC.2019.2936025.
- [3] PAN, C., H. REN, K. WANG, W. XU, M. ELKASHLAN and A. NALLANATHAN. Multicell MIMO Communications Relying on Intelligent Reflecting Surfaces. *IEEE Trans*actions on Wireless Communications. 2020, vol. 19, iss. 8, pp. 5218–5233. ISSN 1536-1276. DOI: 10.1109/TWC.2020.2990766.
- [4] PAN, C., H. REN, K. WANG, M. ELKA-SHLAN, A. NALLANATHAN and J. WANG. Intelligent Reflecting Surface Aided MIMO Broadcasting for Simultaneous Wireless Information and Power Transfer. *IEEE Journal on Selected Areas in Communications*. 2020, vol. 38, iss. 8, pp. 1719–1734. ISSN 0733-8716. DOI: 10.1109/JSAC.2020.3000802.
- [5] ZHANG, S. and R. ZHANG. Capacity Characterization for Intelligent Reflecting Surface Aided MIMO Communication. *IEEE Journal on Selected Areas in Communications*. 2020, vol. 38, iss. 8, pp. 1823–1838. ISSN 0733-8716. DOI: 10.1109/JSAC.2020.3000814.
- [6] ZHOU, G., C. PAN, H. REN, K. WANG, M. DI RENZO and A. NALLANATHAN. Robust Beamforming Design for Intelligent Reflecting Surface Aided MISO Communication Systems. *IEEE Wireless Communications Letters*. 2020, vol. 9, iss. 10, pp. 1658–1662. ISSN 2162-2337. DOI: 10.1109/LWC.2020.3000490.

- [7] TRAN, P. T., B. C. NGUYEN, T. M. HOANG and T. N. NGUYEN. On Performance of Low-Power Wide-Area Networks With the Combining of Reconfigurable Intelligent Surfaces and Relay. *IEEE Transactions on Mobile Computing*. 2022, vol. 22, iss. 10, pp. 6086–6096. ISSN 1536-1233. DOI: 10.1109/TMC.2022.3186394.
- [8] XU, B., T. ZHOU, X. TAO, T. XU and Y. WANG. Ergodic Capacity Analysis for Relay-RIS System Under Three-Dimensional Channel Model. *IEEE Communications Letters*. 2022, vol. 26, iss. 10, pp. 2292–2296. ISSN 1089-7798. DOI: 10.1109/LCOMM.2022.3190295.
- [9] LIANG, X., Q. LIU, W. CAO, S. LIU and X. ZHAO. AoI Minimization for RIS-Assisted V2V Relay System With Deep Reinforcement Learning. *IEEE Internet of Things Journal*. 2025, vol. 12, iss. 14, pp. 27450–27460. ISSN 2327-4662. DOI: 10.1109/JIOT.2025.3564334.
- [10] YI, P., W. CHENG, J. WANG and W. ZHANG. RIS-Assisted Seamless Connectivity in Wireless Multi-Hop Relay Networks. *IEEE Transactions on Mobile Computing*. 2025, pp. 1–13. ISSN 1536-1233. DOI: 10.1109/TMC.2025.3557676.
- [11] WANG, T., F. FANG and Z. DING. An SCA and Relaxation Based Energy Efficiency Optimization for Multi-User RIS-Assisted NOMA Networks. *IEEE Transactions on Vehicular Technology*. 2022, vol. 71, iss. 6, pp. 6843–6847. ISSN 0018-9545. DOI: 10.1109/TVT.2022.3162197.
- [12] VU, T.-H., T. N. NGUYEN, T.-T. NGUYEN and S. KIM. Hybrid Active-Passive STAR-RIS-Based NOMA Systems: Energy/Rate-Reliability Trade-Offs and Rate Adaptation. *IEEE Wireless Communications Letters*. 2025, vol. 14, iss. 1, pp. 238–242. ISSN 2162-2337. DOI: 10.1109/LWC.2024.3497978.
- [13] TRAN, C. H., T. N. NGUYEN, V. Q. SY, A.-T. LE, M. V. BUI and M. VOZNAK. Performance Analysis of Ergodic Rate and Effective Capacity for RIS-Assisted NOMA Networks Over Nakagami-m Fading Environments. *IEEE Access*. 2024, vol. 12, pp. 181271–181281. ISSN 2169-3536. DOI: 10.1109/ACCESS.2024.3509856.
- [14] NGUYEN, Q. S., H.-Y. KIM, T. N. NGUYEN, M. V. BUI, P. T. TRAN, T. T. DUY, B.-S. KIM and M. VOZNAK. Performance of RIS-Secured Short-Packet NOMA Systems With Discrete Phase-Shifter to Protect Digital Content and Copyright Against Untrusted User. *IEEE Access*. 2025, vol. 13, pp. 21580–21593. ISSN 2169-3536. DOI: 10.1109/ACCESS.2025.3535813.

- [15] KHAN, W. U., E. LAGUNAS, A. MAHMOOD, S. CHATZINOTAS and B. OTTERSTEN. RIS-Assisted Energy-Efficient LEO Satellite Communications With NOMA. *IEEE Transactions on Green Communications and Networking*. 2023, vol. 8, iss. 2, pp. 780–790. ISSN 2473-2400. DOI: 10.1109/TGCN.2023.3344102.
- [16] LE, S.-P., T. N. NGUYEN, T. LE-TIEN, T. T. DUY, T.-T. NGUYEN, D. W. K. NG, L.-T. TU and M. VOZNAK. On the Secrecy Performance of Reconfigurable Intelligent Surfaces-Assisted Satellite Networks Under Shadow-Rician Channels. *IEEE Transac*tions on Aerospace and Electronic Systems. 2025, vol. 61, iss. 3, pp. 6794–6808. ISSN 0018-9251. DOI: 10.1109/TAES.2025.3532227.
- [17] FU, S., W. WEI, X. FENG and L. YIN. Average Sum Rate Optimization in RIS-Assisted NOMA Satellite Network: A Deep Reinforcement Learning Approach. *IEEE Wireless Communications Letters*. 2025, vol. 14, iss. 6, pp. 1772–1776. ISSN 2162-2337. DOI: 10.1109/LWC.2025.3555834.
- [18] GUO, K. and K. AN. On the Performance of RIS-Assisted Integrated Satellite-UAV-Terrestrial Networks With Hardware Impairments and Interference. *IEEE Wireless Communications Letters*. 2021, vol. 11, iss. 1, pp. 131–135. ISSN 2162-2337. DOI: 10.1109/LWC.2021.3122189.
- [19] PHAN, V.-D., B. C. NGUYEN, T. M. HOANG, T. N. NGUYEN, P. T. TRAN, M. V. BUI and M. VOZNAK. Performance of Cooperative Communication System With Multiple Reconfigurable Intelligent Surfaces Over Nakagami-m Fading Channels. *IEEE Access*. 2022, vol. 10, pp. 9806–9816. ISSN 2169-3536. DOI: 10.1109/ACCESS.2022.3144364.
- [20] NGUYEN, B. C., T. M. HOANG, P. T. TRAN, T. N. NGUYEN, V.-D. PHAN, M. V. BUI and M. VOZNAK. Cooperative Communications for Improving the Performance of Bidirectional Full-Duplex System With Multiple Reconfigurable Intelligent Surfaces. *IEEE Access*. 2021, vol. 9, pp. 134733–134742. ISSN 2169-3536. DOI: 10.1109/ACCESS.2021.3114713.
- [21] LE, S.-P., T. N. NGUYEN, M. VOZNAK, B. C. NGUYEN, T. M. HOANG, M. V. BUI and P. T. TRAN. Improving the Capacity of NOMA Network Using Multiple Aerial Intelligent Reflecting Surfaces. *IEEE Access.* 2023, vol. 11, pp. 107958–107971. ISSN 2169-3536. DOI: 10.1109/ACCESS.2023.3319675.

- [22] YAN, W., X. YUAN, Z.-Q. HE and X. KUAI. Passive Beamforming and Information Transfer Design for Reconfigurable Intelligent Surfaces Aided Multiuser MIMO Systems. *IEEE Journal on Selected Areas in Communications*. 2020, vol. 38, iss. 8, pp. 1793–1808. ISSN 0733-8716. DOI: 10.1109/JSAC.2020.3000811.
- [23] BASAR, E. Reconfigurable Intelligent Surface-Based Index Modulation: A New Beyond MIMO Paradigm for 6G. IEEE Transactions on Communications. 2020, vol. 68, iss. 5, pp. 3187–3196. ISSN 0090-6778. DOI: 10.1109/TCOMM.2020.2971486.
- [24] DI RENZO, M., K. NTONTIN, J. SONG, F. H. DANUFANE, X. QIAN and F. LAZARAKIS. Reconfigurable Intelligent Surfaces vs. Relaying: Differences, Similarities, and Performance Comparison. *IEEE Open Jour*nal of the Communications Society. 2020, vol. 1, pp. 798–807. ISSN 2644-125X. DOI: 10.1109/OJ-COMS.2020.3002955.
- [25] HUANG, C., A. ZAPPONE, G. C. ALEXAN-DROPOULOS, M. DEBBAH and C. YUEN. Reconfigurable Intelligent Surfaces for Energy Efficiency in Wireless Communication. *IEEE Transactions on Wireless Communications*. 2019, vol. 18, iss. 8, pp. 4157–4170. ISSN 1536-1276. DOI: 10.1109/TWC.2019.2922609.
- [26] NGUYEN, T. N., N. N. THANG, B. C. NGUYEN, T. M. HOANG and P. T. TRAN. Intelligent-Reflecting-Surface-Aided Bidirectional Full-Duplex Communication System With Imperfect Self-Interference Cancellation and Hardware Impairments. *IEEE Systems Journal*. 2023, vol. 17, iss. 1, pp. 1352–1362. ISSN 1932-8184. DOI: 10.1109/JSYST.2022.3167514.
- [27] LE, A.-T., T.-H. VU, T. N. NGUYEN, V. M. BUI and M. VOZNAK. On Performance of Cooperative Satellite-AAV-Secured Reconfigurable Intelligent Surface Systems With Phase Errors. *IEEE Communications Letters*. 2025, vol. 29, iss. 4, pp. 786–790. ISSN 2162-2337. DOI: 10.1109/LCOMM.2025.3543732.
- [28] NGUYEN, T. N., N. V. VINH, B. C. NGUYEN and M. V. BUI. On Performance of RIS-Aided Bidirectional Full-Duplex Systems With Combining of Imperfect Conditions. Wireless Networks. 2024, vol. 30, pp. 649–660. DOI: 10.1007/s11276-023-03490-7.
- [29] ZHAI, X., G. HAN and Y. CAI. Robust Design of RIS-Assisted Over-the-Air Computation in the Face of Long-Term and Short-Term Imperfections. IEEE Transactions on Vehicular Technology.

- 2024, vol. 73, iss.11, pp. 16817–16831. ISSN 0018-9545. DOI: 10.1109/TVT.2024.3419807.
- [30] HOANG, T. M., B. C. NGUYEN, N. N. THANG, M. TRAN and P. T. TRAN. Performance and Optimal Analysis of Time-Switching Energy Harvesting Protocol for MIMO Full-Duplex Decode-and-Forward Wireless Relay Networks With Various Transmitter and Receiver Diversity Techniques. *Journal of the Franklin Insti*tute. 2020, vol. 357, iss. 17, pp. 13205–13230. DOI: 10.1016/j.jfranklin.2020.09.037.
- [31] LE, A.-T., T.-H. VU, T. N. NGUYEN, T. L.-TIEN and M. VOZNAK. Partial Multiplexing Power-Frequency Multiple Access for Active STAR-RIS Systems: Outage and Ergodic Perspectives. *IEEE Wireless Communications Let*ters. 2025, vol. 14, iss. 3, pp. 799–803. ISSN 1089-7798. DOI: 10.1109/LCOMM.2025.3543732.
- [32] ROSTAMI GHADI, F. and F. J. LÓPEZ-MARTÍNEZ. RIS-Aided Communications Over Dirty MAC: Capacity Region and Outage Probability. *IEEE Communications Letters*. 2023, vol. 27, iss. 8, pp. 2009–2013. ISSN 1089-7798. DOI: 10.1109/LCOMM.2023.3284502.
- [33] LU, H., Y. CHEN and N. CAO. Accurate Approximation to the PDF of the Product of Independent Rayleigh Random Variables. *IEEE Antennas and Wireless Propagation Letters*. 2011, vol. 10, pp. 1019–1022. ISSN 1536-1225. DOI: 10.1109/LAWP.2011.2168938.
- [34] CHANDRAMOULI, R. and N. RAN-GANATHAN. Computing the bivariate Gaussian probability integral. *IEEE Signal Processing Letters*. 1999, vol. 6, iss. 6, pp. 129–131. ISSN 1070-9908. DOI: 10.1109/97.763142.
- [35] BADIU, M.-A. and J. P. COON. Communication Through a Large Reflecting Surface With Phase Errors. *IEEE Wireless Communications Letters*. 2019, vol. 9, iss. 2, pp. 184–188. ISSN 2162-2337. DOI: 10.1109/LWC.2019.2947445.

Appendix A Proofs of Lemmas 1–4

For Rayleigh fading channels, the probability density function (PDF) is given by $f(x, \sigma) = \frac{x}{\sigma^2} \exp\left(-\frac{x^2}{2\sigma^2}\right)$, for $x \ge 0$, $\sigma > 0$ [33].

$$E\{X\} = \int_{0}^{\infty} x f(x,\sigma) dx$$

$$= \int_{0}^{\infty} x \cdot \frac{x}{\sigma^{2}} \exp\left(-\frac{x^{2}}{2\sigma^{2}}\right) dx \qquad (12)$$

$$= \frac{1}{\sigma^{2}} \int_{0}^{\infty} x^{2} \exp\left(-\frac{x^{2}}{2\sigma^{2}}\right) dx$$

We apply integration by parts. Let

$$u = x$$
, $dv = x \exp\left(-\frac{x^2}{2\sigma^2}\right) dx$.

Then

$$du = dx$$
, $v = -\sigma^2 \exp\left(-\frac{x^2}{2\sigma^2}\right)$.

Substituting back into equation (12), we have:

$$\begin{aligned} \mathbf{E}\{X\} &= \frac{1}{\sigma^2} \left(uv \Big|_0^\infty - \int_0^\infty v \, du \right) \\ &= \frac{1}{\sigma^2} \left[x \left(-\sigma^2 \exp\left(-\frac{x^2}{2\sigma^2} \right) \right) \Big|_0^\infty \right. \\ &\left. + \sigma^2 \int_0^\infty \exp\left(-\frac{x^2}{2\sigma^2} \right) dx \right] \\ &= \int_0^\infty \exp\left(-\frac{x^2}{2\sigma^2} \right) dx \end{aligned} \tag{13}$$

Let $u = \frac{x}{\sqrt{2}\sigma} \Rightarrow du = \frac{1}{\sqrt{2}\sigma}dx$, then:

$$E\{X\} = \sqrt{2}\sigma \int_0^\infty \exp(-u^2)du$$
 (14)

Using the Gaussian integral [34],

$$\int_{-\infty}^{\infty} \exp(-x^2) dx = \sqrt{\pi},$$

and noting that the function is symmetric, we find:

$$\int_0^\infty \exp(-x^2) dx = \frac{\sqrt{\pi}}{2}$$

Thus,

$$E\{X\} = \sqrt{2}\sigma \cdot \frac{\sqrt{\pi}}{2} = \sigma\sqrt{\frac{\pi}{2}}$$
 (15)

This is the expected value of a Rayleigh-distributed random variable.

Next, assume that the phase error Θ_n follows a uniform distribution over the interval $\left[-\frac{\Delta}{2},\frac{\Delta}{2}\right]$, with $\Delta=\frac{2\pi}{2^q}$, where q is the number of quantization bits.

The corresponding PDF is:

$$f_{\Theta_n}(x) = \begin{cases} \frac{1}{\Delta}, & x \in \left[-\frac{\Delta}{2}, \frac{\Delta}{2}\right] \\ 0, & \text{otherwise} \end{cases}$$

The expected value of the phase term is given by:

$$\begin{split} \mathrm{E}\left\{\exp\left(-j\Theta_{n}\right)\right\} &= \int_{-\frac{\Delta}{2}}^{\frac{\Delta}{2}} \exp(-j\Theta_{n}) \cdot \frac{1}{\Delta} d\Theta_{n} \\ &= \frac{-1}{\Delta j} \left(\exp\left(-j\frac{\Delta}{2}\right) - \exp\left(j\frac{\Delta}{2}\right)\right) \end{split} \tag{16}$$

Using Euler's identity:

$$\exp(-j\alpha) - \exp(j\alpha) = -2j\sin(\alpha)$$

with $\alpha = \frac{\Delta}{2}$, we get:

$$E\left\{\exp\left(-j\Theta_n\right)\right\} = \frac{2\sin\left(\frac{\Delta}{2}\right)}{\Delta} = \operatorname{sinc}\left(\frac{\Delta}{2}\right) = \operatorname{sinc}\left(\frac{\pi}{2^q}\right)$$
(17)

Now consider a Rayleigh-distributed random variable X, with PDF $f(x;\sigma)=\frac{x}{\sigma^2}\exp\left(-\frac{x^2}{2\sigma^2}\right),\ x\geq 0$. Its second moment is:

$$E\{X^2\} = \int_0^\infty x^2 f(x;\sigma) dx = \frac{1}{\sigma^2} \int_0^\infty x^3 \exp\left(-\frac{x^2}{2\sigma^2}\right) dx$$
(18)

Let $u = x^2 \Rightarrow du = 2x dx$, then:

$$E\{X^2\} = \frac{1}{2\sigma^2} \int_0^\infty u \exp\left(-\frac{u}{2\sigma^2}\right) du \tag{19}$$

Using $t = \frac{u}{2\sigma^2} \Rightarrow du = 2\sigma^2 dt$, we obtain:

$$E\{X^2\} = 2\sigma^2 \int_0^\infty t \exp(-t)dt \tag{20}$$

Using integration by parts with u = t, $dv = \exp(-t)dt$, $v = -\exp(-t)$, we find:

$$E\{X^{2}\} = 2\sigma^{2} \left[uv \Big|_{0}^{\infty} - \int_{0}^{\infty} v \, du \right] = 2\sigma^{2}(0+1) = 2\sigma^{2}$$
(21)

Next, we evaluate $\operatorname{E}\left\{\exp\left(j\theta_{n}\right)^{2}\right\} \equiv \operatorname{E}\left\{\exp\left(-j\Theta_{n}\right)^{2}\right\}$. While some previous works assume this value equals 1, this assumption is physically inaccurate, as practical phase errors distort the signal [35]. Thus, we take the real part to accurately

capture the degradation due to phase errors:

$$E\left\{\exp\left(-j\Theta_{n}\right)^{2}\right\} = E\left\{\cos\left(2\Theta_{n}\right) - j\sin\left(2\Theta_{n}\right)\right\}$$

$$= E\left\{\cos\left(2\Theta_{n}\right)\right\} - jE\left\{\sin\left(2\Theta_{n}\right)\right\}$$

$$= \int_{-\frac{\Delta}{2}}^{\frac{\Delta}{2}} \cos\left(2\Theta_{n}\right) \frac{1}{\Delta} d_{\Theta_{n}}$$

$$- j \int_{-\frac{\Delta}{2}}^{\frac{\Delta}{2}} \sin\left(2\Theta_{n}\right) \frac{1}{\Delta} d_{\Theta_{n}}$$

$$= \frac{1}{\Delta} \left(\frac{\sin\left(2\Theta_{n}\right)}{2}\Big|_{-\frac{\Delta}{2}}^{\frac{\Delta}{2}}\right)$$

$$+ j \left(\frac{\cos\left(2\Theta_{n}\right)}{2}\Big|_{-\frac{\Delta}{2}}^{\frac{\Delta}{2}}\right)$$

$$= \frac{1}{\Delta} \left(\frac{\sin\left(\Delta\right) - \sin\left(-\Delta\right)}{2}\right)$$

$$+ j \left(\frac{\cos\left(\Delta\right) - \cos\left(-\Delta\right)}{2}\right)$$

$$= \frac{1}{\Delta} \left(\frac{2\sin\left(\Delta\right)}{2} + j\left(0\right)\right)$$

$$= \frac{\sin\left(\Delta\right)}{\Delta} = sinc\left(\Delta\right)$$
(22)

From the above analytical results, we can formally establish the four lemmas as follows:

- Lemmas 1 and 3 are obtained in a straightforward manner by substituting the expectations given in (15) and (17) into the definitions of Z.
- Lemmas 2 and 4, on the other hand, require combining the statistical properties provided in (15), (17), (21), and (22), which describe the first- and second-order moments of the fading channels and the phase shift errors of the RIS.

Specifically, for Lemma 1, we have

$$E\{Z\} = E\left\{\sum_{k=1}^{K} h_{S,D_{k}} + \sum_{k=1}^{K} \sum_{n=1}^{N} h_{S,RIS} \exp(j\theta_{n}) h_{RIS,D_{k}}\right\}$$

$$= E\left\{\sum_{k=1}^{K} h_{S,D_{k}}\right\}$$

$$+ E\left\{\sum_{k=1}^{K} \sum_{n=1}^{N} h_{S,RIS} \exp(j\theta_{n}) h_{RIS,D_{k}}\right\},$$
(23)

where the first term corresponds to the direct transmission links, while the second term represents the average contribution of the cascaded RIS-assisted links.

For Lemma 3, considering the case of a single destination, the expectation reduces to

$$E\{Z\} = E\left\{h_{S,D_k} + \sum_{n=1}^{N} h_{S,RIS} \exp(j\theta_n) h_{RIS,D_k}\right\}$$
$$= E\{h_{S,D_k}\} + E\left\{\sum_{n=1}^{N} h_{S,RIS} \exp(j\theta_n) h_{RIS,D_k}\right\}.$$
(24)

This expression highlights the decomposition of the expectation into the direct link and the RIS-assisted reflection links.

Next, for Lemma 2, we characterize the variance of Z as

$$\operatorname{Var}\{Z\} = \operatorname{Var}\left\{\sum_{k=1}^{K} h_{S,D_{k}} + \sum_{k=1}^{K} \sum_{n=1}^{N} h_{S,RIS} \exp(j\theta_{n}) h_{RIS,D_{k}}\right\}$$

$$= \operatorname{Var}\left\{\sum_{k=1}^{K} h_{S,D_{k}}\right\} + \operatorname{Var}\left\{\sum_{k=1}^{K} \sum_{n=1}^{N} h_{S,RIS} \exp(j\theta_{n}) h_{RIS,D_{k}}\right\}$$

$$= K\left(\operatorname{E}\{h_{S,D_{k}}^{2}\} - \left(\operatorname{E}\{h_{S,D_{k}}\}\right)^{2}\right)$$

$$+ KN\left(\operatorname{E}\{(h_{S,RIS} \exp(j\theta_{n}) h_{RIS,D_{k}})^{2}\}\right)$$

$$- \left(\operatorname{E}\{h_{S,RIS} \exp(j\theta_{n}) h_{RIS,D_{k}}\}\right)^{2}\right). \tag{25}$$

The above decomposition clearly separates the variance due to direct links and that due to cascaded RIS-assisted channels, scaled by the number of terminals K and the number of reflecting elements N.

Finally, for Lemma 4, when considering only one destination, we obtain

$$\operatorname{Var}\{Z\} = \operatorname{Var}\left\{h_{S,D_{k}} + \sum_{n=1}^{N} h_{S,RIS} \exp(j\theta_{n}) h_{RIS,D_{k}}\right\}$$

$$= \operatorname{Var}\{h_{S,D_{k}}\} + \operatorname{Var}\left\{\sum_{n=1}^{N} h_{S,RIS} \exp(j\theta_{n}) h_{RIS,D_{k}}\right\}$$

$$= \left(\operatorname{E}\{h_{S,D_{k}}^{2}\} - \left(\operatorname{E}\{h_{S,D_{k}}\}\right)^{2}\right)$$

$$+ N\left(\operatorname{E}\{(h_{S,RIS} \exp(j\theta_{n}) h_{RIS,D_{k}})^{2}\}\right)$$

$$- \left(\operatorname{E}\{h_{S,RIS} \exp(j\theta_{n}) h_{RIS,D_{k}}\}\right)^{2}. (26)$$

It is important to emphasize that the required expectations, namely $\mathbb{E}\{h_{S,RIS}\}$, $\mathbb{E}\{h_{S,D_k}\}$, and $\mathbb{E}\{h_{RIS,D_k}\}$, are directly obtained from (15), whereas $\mathbb{E}\{h_{S,RIS}^2\}$, $\mathbb{E}\{h_{S,D_k}^2\}$, and $\mathbb{E}\{h_{RIS,D_k}^2\}$ are provided in (21). Furthermore, the statistical characterization of the phase noise, i.e., $\mathbb{E}\{\exp(j\theta_n)\}$ and $\mathbb{E}\{\exp(j\theta_n)^2\}$, is given in (17) and (22), respectively. By incorporating these relations, Lemma 2 is rigorously derived, while Lemma 4 naturally follows by omitting the summation $\sum_{k=1}^K$. This completes the proof of Lemmas 1–4.